

TANGENTIAL RETINAL DISPLACEMENT INCREASES AFTER MACULAR PUCKER SURGERY

An Apparent Nonsense

TOMMASO ROSSI, MD,* GIORGIO QUERZOLI, PhD,† PAMELA COSIMI, MD,* GUIDO RIPANDELLI, MD,* DAVID H. STEEL, MD,‡ MARIO R. ROMANO, MD, PhD§

Purpose: To measure the tangential retinal displacement and vision before and after macular pucker surgery and study if pars plana vitrectomy with epiretinal membrane peeling allows the reconstitution of previous anatomy or else it results in a different configuration.

Methods: Retrospective series of patients undergoing pars plana vitrectomy for epiretinal membrane, with >6-month follow-up before and after surgery, complete with best-corrected visual acuity, optical coherence tomography, M-Charts, and infrared retinography. Tangential retinal displacement between earliest visit (T_E), time of surgery (T_0), and latest available visit (T_L) of the examined retina, concentric circles at 0.5, 1.5, and 4.5 mm radii, and the central horizontal and vertical meridians were measured. Tangential displacement was calculated as the optical flow of consecutive infrared photographs.

Results: The study comprised 32 patients: 15 men and 17 women. Average preoperative and postoperative follow-up were 23.4 ± 27.9 months and 19.2 ± 11.8 months, respectively. Best-corrected visual acuity reduced before surgery (0.69 ± 0.16 Snellen to 0.46 ± 0.17 ; $P < 0.001$) and increased after (0.866 ± 0.16 Snellen; $P < 0.001$). Horizontal and vertical metamorphopsia increased between before surgery but only horizontal metamorphopsia significantly reduced after. Average tangential displacement before surgery was $35.6 \pm 29.9 \mu\text{m}$ versus $56.6 \pm 41.3 \mu\text{m}$ after ($P = 0.023$). Preoperative and postoperative displacement within the fovea was less than over the entire area ($P < 0.001$).

Conclusion: Retinal tangential displacement between diagnosis and surgery ($T_E - T_0$) is less than the displacement occurring after surgery ($T_0 - T_L$). Postoperative displacement does not represent the restoration of the anatomy existing before the disease ensued but rather the resulting equilibrium of newly deployed forces.

RETINA 44:610–617, 2024

Primary epiretinal membranes (ERMs) may form after anomalous posterior vitreous detachment when hyalocytes and other preretinal cells in remnants of the adherent posterior hyaloid develop contractile properties and deform the retina.¹ Although classified as a vitreo-retinal interface disease, ERMs cause profound alterations of both the inner and the outer retinal layers,² especially in the later stages.

Pars plana vitrectomy with ERM peeling, variably associated with internal limiting membrane (ILM) removal,³ can stop and often reverse visual deterioration and are widely regarded as an effective treatment for symptomatic ERMs. Despite symptomatic

improvement, the ultrastructural changes associated with the pathogenic process and the restorative mechanisms after surgery remain poorly understood.^{4,5}

We recently described a novel image analysis technique aimed at calculating the map of the displacements in consecutive retinal images and used it to study the postoperative en face retinal distortion after ERM peeling.⁶

The present study aims at reporting retinal displacement and vision function throughout the course of disease, starting well before surgery was deemed necessary, shortly after the diagnosis of ERM was made, and after surgery with a lengthy postoperative

follow-up. The purpose is to observe if and to what extent the surgical removal of ERMs reestablishes the previous pre-morbid ultrastructural anatomy or rather it results in a new and different configuration, shaped by the balance of forces established after the surgery.

Materials and Methods

Study Participants

We retrospectively analyzed the records of all patients undergoing pars plana vitrectomy and peeling for idiopathic ERM affecting the fovea and classified as Stage 2 to 3 according to Govetto et al⁷ with documented preoperative and postoperative follow-up >6 months (i.e., before and after surgery). The number of patients whose data were available per time interval before and after surgery is reported in Table 1.

All patients received surgery at the IRCCS Bietti Foundation between January 2019 and June 2022 and had been operated by a single surgeon. Diagnosis was confirmed by ophthalmoscopic examination and spectral-domain optical coherence tomography.

Exclusion criteria were as follows: 1) history of ocular and specifically macular disorders including age-related macular degeneration, retinal vascular occlusions, retinal detachment, trauma, high myopia (ocular axial length >26.00 mm), and uveitis; 2) history of systemic diseases, including hypertension and diabetes; 3) poor imaging quality because of media opacity; and 4) incomplete medical records.

All patients had at least three visits before and three visits after surgery. At each visit, they had a full refraction, best-corrected visual acuity (BCVA) using Early Treatment Diabetic Retinopathy Study acuity charts and Snellen visual acuity converted to the logarithm of minimum angle of resolution units for statistical purposes and indirect ophthalmoscopy performed. The degree of horizontal and vertical metamorphopsia was assessed via M-Charts (Inami, Co, Tokyo, Japan).⁸

From the *IRCCS—Fondazione Bietti ONLUS, Roma, Italy; †DI-CAAR Faculty of Engineering, University of Cagliari, Cagliari, Italy; ‡Newcastle University, Newcastle, United Kingdom; and §Department of Biomedical Science, Humanitas University, Milan, Italy.

None of the authors has any financial/conflicting interests to disclose.

This is an open access article distributed under the terms of the Creative Commons Attribution-Non Commercial-No Derivatives License 4.0 (CCBY-NC-ND), where it is permissible to download and share the work provided it is properly cited. The work cannot be changed in any way or used commercially without permission from the journal.

Reprint requests: Tommaso Rossi, MD, IRCCS Fondazione Bietti ONLUS, Via Livorno 3, Roma 00198, Italy; e-mail: tommaso.rossi@usa.net

Table 1. Number of Patients Available at Each Time Interval

<T ₋₁₂	T ₋₁₂	T ₋₆	T ₋₀	T ₊₃	T ₊₆	T ₊₁₂	T ₊₁₈	>T ₊₁₈
12	19	32	32	32	32	31	18	11

For the purpose of the present study, we defined T_E as the very first available preoperative office visit, T₀ as the visit immediately before surgery (within 7 days), and T_L as the very last available postoperative visit. All patients provided written informed consent; the study adhered to the tenets of the Declaration of Helsinki and received approval of the local Ethics Committee (ERMLAB01 N° 77/18/FB).

Surgical Procedure

All patients underwent a standard 25-gauge, 3-port pars plana vitrectomy (using BVI R-Evolution CR800; BVI Medical, Waltham, MA) with ERM and ILM peeling with single Brilliant Blue G staining (Monoblue, BVI Medical).

Optical Coherence Tomography Image Acquisition

Optical coherence tomography images were acquired using the horizontal spectral-domain optical coherence tomography cross-section (an average of 25–30 frames for each B-scan was used to improve image quality as elsewhere reported, using Heidelberg Spectralis, Heidelberg, Germany⁹).

En Face Displacement Measures

En face dislocation was evaluated by measuring the displacement occurring between pairs of successive infrared 9 × 9-mm²-wide images acquired as spectral-domain optical coherence tomography (Spectralis HRA-OCT, version 1.5.12.0; Heidelberg Engineering, Heidelberg, Germany) by means of an optical flow algorithm described elsewhere.⁶ The present study analyzed the displacements occurring during the preoperative period (T_E – T₀), the postoperative period (T₀ – T_L), and the entire course of observation (T_E – T_L).

Briefly, the gray images were inverted, and their details were enhanced by adjusting locally each image to obtain a flat intensity histogram. The displacements were measured on a regular grid, using the Farneback two-frame motion estimation method,¹⁰ then a roto-translation was subtracted to align the two images. Finally, the aligned images were further analyzed to measure the retinal displacements in microns, and the statistics such as mean values were computed using

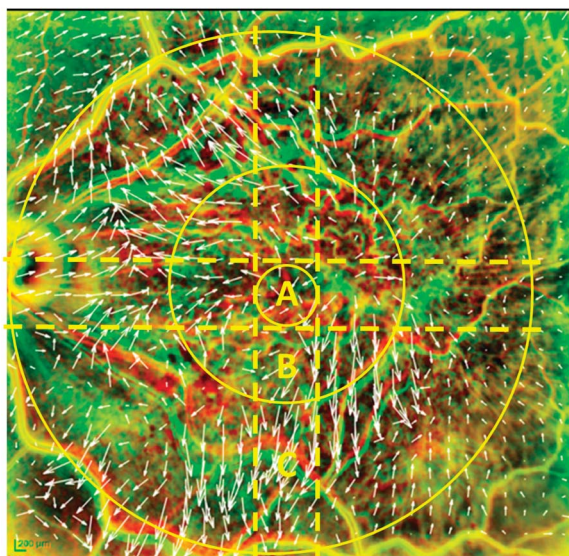


Fig. 1. Regions used to analyze the retinal deformation in $T_0 - T_E$ example image. The yellow lines indicate: (A) the “central” circular region 0.5 mm in radius; (B) the “perifoveal” region 1.5 mm in radius; (C) the “parafoveal” region 4.5 mm in radius. The dashed lines indicate the horizontal and vertical 1-mm-wide regions constituting the “cross-hair” region where M-Charts project.

the displacement magnitude of the vectors $D = \sqrt{D_x^2 + D_y^2}$ included in the region of interest.

We analyzed the results (shown as vector fields): 1) over the whole image; 2) in a crosshair region consisting of the union of the 1-mm-wide areas adjacent to a horizontal and a vertical line crossing on the foveola (horizontal and vertical meridian, respectively) and corresponding to the region where the M-Charts lines retinal image forms (Figure 1); 3) over three circular regions centered on the foveola with radii equal to 0.5, 1.5, and 4.5 mm (indicated in Figure 1 with A, B, and C, respectively).

Additionally, the horizontal and vertical component, D_x and D_y , of the displacement vectors across the entire $9 \times 9 \text{ mm}^2$ area and within the crosshair region formed by the two 1-mm-wide above-mentioned regions were evaluated to calculate the predominant component, respectively, during the $(T_E - T_0)$, $(T_0 - T_L)$, or $(T_E$

$- T_L)$ periods: a displacement was considered predominantly horizontal or vertical when the $D_x > D_y$ or $D_y > D_x$, respectively. Therefore, displacement vectors at angles comprised in the ranges $\pm 45^\circ$ or 135° to 225° (i.e., $\pm \pi/4$ or $3/4\pi \pm \pi/4$; horizontal meridian is conventionally attributed 0°) were prevalently horizontal, whereas vector angles comprised in the ranges 45° to 135° or 225° to 315° (i.e., $\pi/2 \pm \pi/4$ and $3/2\pi \pm \pi/4$) had a prevalent vertical component. This has been done to test correlation with M-Charts scoring and to account for retinal anisotropy.

Main Outcome Measures

The main study outcome measures were BCVA, M-Charts grading, foveal thickness, and mean retinal displacement.

Statistical Analysis

Analysis of variance with *t*-test and *t*-test for repeated measures applied to numerical variables were used to assess changes at different time-points. Bivariate Pearson *r* correlation coefficient was applied for continuous variables, whereas Spearman rho and Kendall Tau were used for the assessment of ordinal variables. Shapiro–Wilk test was used for the Gaussian distribution of data. In all cases, *P* values < 0.05 were considered statistically significant.

Results

Visual Acuity, Microperimetry and Metamorphopsia

Thirty-two patients (15 men and 17 women) satisfied the inclusion criteria; mean age was comparable between the sexes: 74.1 ± 10.1 years for men and 72.1 ± 8.2 for women.

Average preoperative follow-up was 23.4 ± 27.9 months (range 6–84 months; median 8 months, interquartile range 15.5 months), and average postoperative follow-up was 19.2 ± 11.8 months (range 6–48

Table 2. Main Clinical Outcome Measures: BCVA (Snellen Fraction and Logarithm of Minimum Angle of Resolution), Foveal Thickness, Vertical and Horizontal Metamorphopsias, and Retinal Sensitivity at the Earliest Visit, T_0 , and the Latest Visit

	T_E	T_0	<i>P</i> (T_E vs. T_0)	T_L	<i>P</i> (T_0 vs. T_L)
BCVA (Snellen)	0.69 ± 0.16	0.46 ± 0.17	< 0.001	0.86 ± 0.16	< 0.001
BCVA (logMAR)	0.16 ± 0.79	0.33 ± 0.76	< 0.001	0.06 ± 0.79	< 0.001
OCT foveal thickness (μm)	450.1 ± 110.6	460.7 ± 125.2	n.s.	386.3 ± 61.8	0.003
Horizontal metamorphopsia ($^\circ$)	0.36 ± 0.23	1.15 ± 0.79	< 0.001	0.67 ± 0.62	< 0.001
Vertical metamorphopsia ($^\circ$)	0.37 ± 0.18	0.89 ± 0.77	< 0.001	0.81 ± 0.61	n.s.

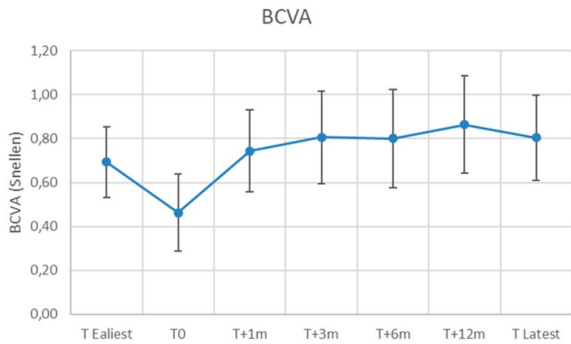


Fig. 2. Best-corrected visual acuity during follow-up note the decrease between the earliest visit (T_E) and the time of surgery (T_0) and subsequent recovery.

months; median 13 months, interquartile range 12 months).

Visual acuity is reported in Table 2 and Figure 2 and significantly reduced from T_E to T_0 (0.69 ± 0.16 Snellen to 0.46 ± 0.17 ; $P < 0.001$) to increase between T_0 and T_L (0.866 ± 0.16 Snellen; $P < 0.001$).

Foveal thickness (Table 2, Figure 3) slightly (but not significantly) increased between T_E and T_0 , whereas it significantly reduced between T_0 and T_L ($P < 0.01$).

Both horizontal and vertical metamorphopsia increased between T_E and T_0 (Table 2 and Figure 4) but only the horizontal metamorphopsia significantly reduced after surgery ($T_0 - T_L$).

En Face Retinal Displacement

The average retinal en face displacement occurring over the entire investigated area before surgery ($T_E - T_0$) was $35.6 \pm 29.9 \mu\text{m}$ versus $56.6 \pm 41.3 \mu\text{m}$ after surgery ($T_0 - T_L$), $P = 0.023$ (Table 3).

The average foveal displacement both preoperative ($T_0 - T_E$) and postoperative ($T_L - T_0$) was signifi-

cantly less than over the entire area: $14 \pm 37.4 \mu\text{m}$ ($P < 0.016$) and $18.1 \pm 44.9 \mu\text{m}$ ($P < 0.001$), respectively.

The retinal en face displacement between T_E and T_L within the central 0.5 mm radius and 1.5 mm annular region was significantly lower than the displacement occurring throughout the entire $9 \times 9 \text{ mm}^2$ area (Table 3; $P < 0.05$ for both).

En face displacement between T_E and T_0 correlated to optical coherence tomography thickness increase during the same preoperative time ($P = 0.018$), whereas it did not correlate to either metamorphopsia increase or BCVA decrease. En face displacement between T_L and T_0 did not significantly correlate to optical coherence tomography thickness, BCVA, or metamorphopsia changes.

Postoperative en face displacement ($T_0 - T_L$) and throughout follow-up ($T_E - T_L$) showed a normal distribution ($P < 0.01$), whereas the displacement in the preoperative period ($T_E - T_0$) did not.

Preoperative ($T_E - T_0$) and postoperative ($T_0 - T_L$) vertical metamorphopsia changes showed a significant correlation with the respective horizontal retinal displacement of the crosshair region showed in Figure 1, where the M-Charts lines project ($P < 0.001$ for both).

The horizontal and vertical components of displacement vectors of the entire $9 \times 9 \text{ mm}^2$ central area showed an erratic orientation (Table 3) with no obvious preponderance of vertical or horizontal components. The 1-mm-wide crosshair region, spanning 9 mm in width and height, showed a gradient of displacement like the adjacent retina and increasing with eccentricity. However, if vectors displacement falling within the 1-mm-wide crosshair were decomposed into their orthogonal components (Figure 5), the horizontal and vertical component of the horizontal strip displaced less in the preoperative

Foveal Thickness

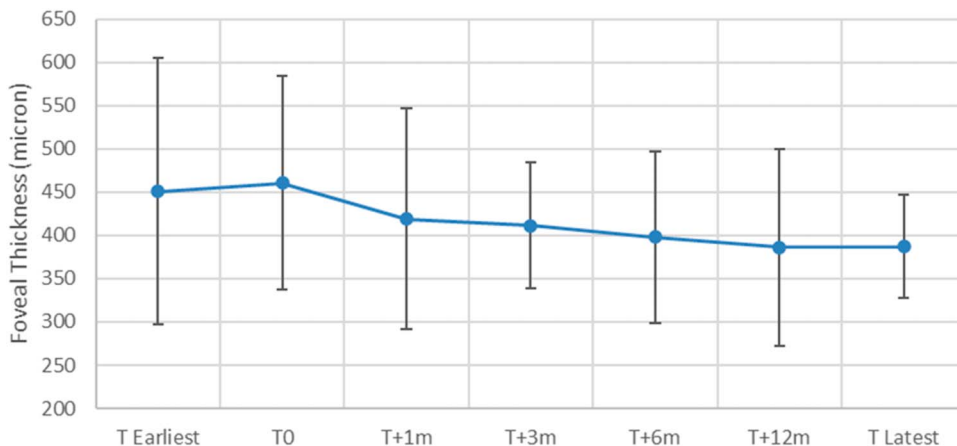
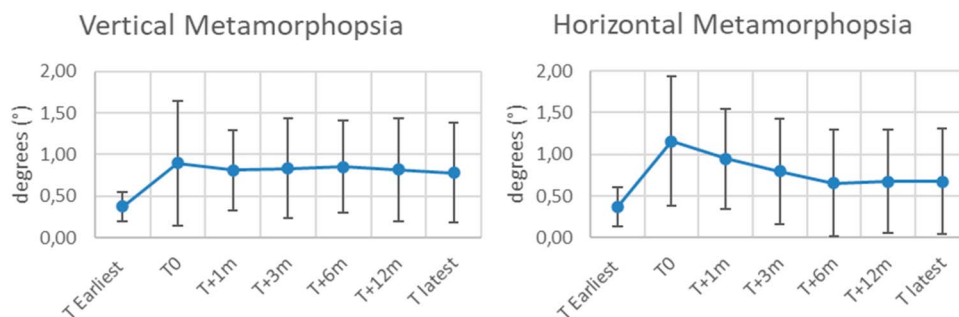


Fig. 3. Foveal thickness during follow-up.

Fig. 4. Vertical (A) and horizontal (B) metamorphopsia during follow-up.



period ($T_E - T_0$) than in the postoperative period ($T_0 - T_L$; Table 4), and both displaced significantly less than any other considered retinal area (analysis of variance; Table 4; $P < 0.01$).

Discussion

Retinal deformation is the hallmark of vitreoretinal interface syndromes, and surgery is intended to correct the pathogenic mechanism to allow anatomical and functional restoration. However, given the inconsistent association between anatomical and functional changes,¹¹ surgery is more often based on vision loss and increase of metamorphopsia than on observed retinal displacement.

The present study used the same method previously described as an objective measure of retinal tangential dislocation after ERM peeling⁶ and extended its application to the preoperative period, immediately after the diagnosis of ERM and well before a decision for surgery was made. Although the exact time of onset of ERMs is virtually impossible to define, including a lengthy preoperative follow-up allowed us to study a prolonged period of the disease, including the changes leading to surgery.

Both BCVA, foveal thickness, and metamorphopsia significantly worsened between T_E and T_0 (Table 2, and Figures 2 and 3), prompting surgical indication. The postoperative results of our series match most of the current literature, in vision gain, foveal thickness

reduction, and horizontal metamorphopsia improvement¹² (Table 2).

Vertical metamorphopsia did not improve significantly after surgery (Table 2), a notion somewhat difficult to explain, already observed by Mieno et al.¹³ and even by Amsler¹⁴ back in 1953 who also reported a greater deformation for horizontal compared with vertical lines. It is worth mentioning that to perceive as “distorted” a horizontal line, the points that compose it must be dislocated vertically and vice versa; therefore, horizontal dislocation mostly affects vertical lines perception, whereas vertical dislocation does the opposite, an observation already proposed by Ichigawa et al.¹⁵

Interestingly, the average macular displacement occurring between diagnosis and surgery ($T_E - T_0$), and theoretically representing the very reason for treatment, is less than the one occurring after surgery ($T_0 - T_L$; Table 3). In other words, the retina deforms more after the surgery than before (Figure 6). Even more puzzling, the average displacement of $65 \mu\text{m}$ (Table 3) between the first and the last visit ($T_E - T_L$) shows that the postoperative displacement by no means represents a “rewinding” of the preoperative pathogenic mechanism. There is no restoration of the former “healthy” anatomy; the resulting new retinal architecture simply represents a balance of the new forces released after ERM (and ILM) peeling reaching a new and different equilibrium, likely characterized by lower internal stresses in the tissue (Figure 6).

Then why and how do vision and metamorphopsias improve? If the retina does not reestablish previous

Table 3. Average En Face Retinal Displacement Vector (in μm) of the Entire $9 \times 9 \text{ mm}^2$ Area and Concentric Circles Centered on the Foveola

	$T_0 - T_E$	$T_L - T_0$	<i>P</i>	$T_L - T_E$
Entire $9 \times 9 \text{ mm}^2$ area	35.6 ± 29.9	56.6 ± 41.3	<0.05	65.0 ± 42.0
Region A: $R < 0.5 \text{ mm}$	14.0 ± 37.4	18.1 ± 44.9	n.s.	14.8 ± 68.1
Region B: $R < 1.5 \text{ mm}$	16.3 ± 42.4	23.7 ± 46.6	n.s.	26.5 ± 63.8
Region C: $R < 4.5 \text{ mm}$	22.7 ± 44.6	37.6 ± 57.4	n.s.	39.9 ± 69.0
Vertical foveal strip 1 mm	30.0 ± 33.3	48.6 ± 34.2	<0.01	60.3 ± 47.7
Horizontal foveal strip 1 mm	31.9 ± 34.5	41.7 ± 36.7	<0.05	54.5 ± 42.8

The 1-mm-wide crosshair region centered on the fovea has been divided into vertical and horizontal foveal strips.

Table 4. Overall Horizontal and Vertical Displacement Vector Decomposition of the Entire 6 × 6 mm² Area and 1-mm-Wide Central Crosshair

	$T_0 - T_E$	$T_L - T_0$	<i>P</i>	$T_L - T_E$
Overall horizontal displacement	20.8 ± 29.1	36.4 ± 35.1	0.049*	38.3 ± 37.0
Overall vertical displacement	21.5 ± 28.6	40.1 ± 40.5	0.037*	42.6 ± 41.2
Horizontal foveal strip horizontal displacement	18.5 ± 26.0	26.0 ± 47.1	0.043*	33.6 ± 35.6
Horizontal foveal strip vertical displacement	6.1 ± 38.4	26.6 ± 29.6	<0.001*	10.9 ± 45.2
Vertical foveal strip horizontal displacement	14.1 ± 17.5	23.8 ± 23.8	0.06	29.2 ± 31.8
Vertical foveal strip vertical displacement	21.4 ± 30.1	29.5 ± 28.5	0.27	38.3 ± 40.5

Note that the central crosshair has been divided into its horizontal and vertical strips and for displacement vectors belonging to each strip decomposed into their respective orthogonal horizontal and vertical components.

*Statistically significant difference.

anatomy but dislocates even more, why does function improve?

Most likely, ERM peeling releases the internal tension of the retina and the cellular elements regain a better function, possibly because of a reduction of kinking at the level of bipolar, ganglion, and Müller cells¹⁶ and the reduced interference with cytokines production and signal transduction.¹⁷

What are the forces that shape preoperative and postoperative retinal architecture?

Vessels and, specifically, the vascular arcades contained in the superficial vascular plexus represent the stiffer retinal structure¹⁸ together with the ILM, whereas Müller cells transect all retinal layers contributing to the layered anatomy.¹⁹ Our data (Tables 3 and 4) showed the erratic disposition of dislocation vectors throughout the macula with the notable exception of the crosshair centered on the fovea: the vertical dislocation of the horizontal arm and horizontal dislocation of the vertical arm are less

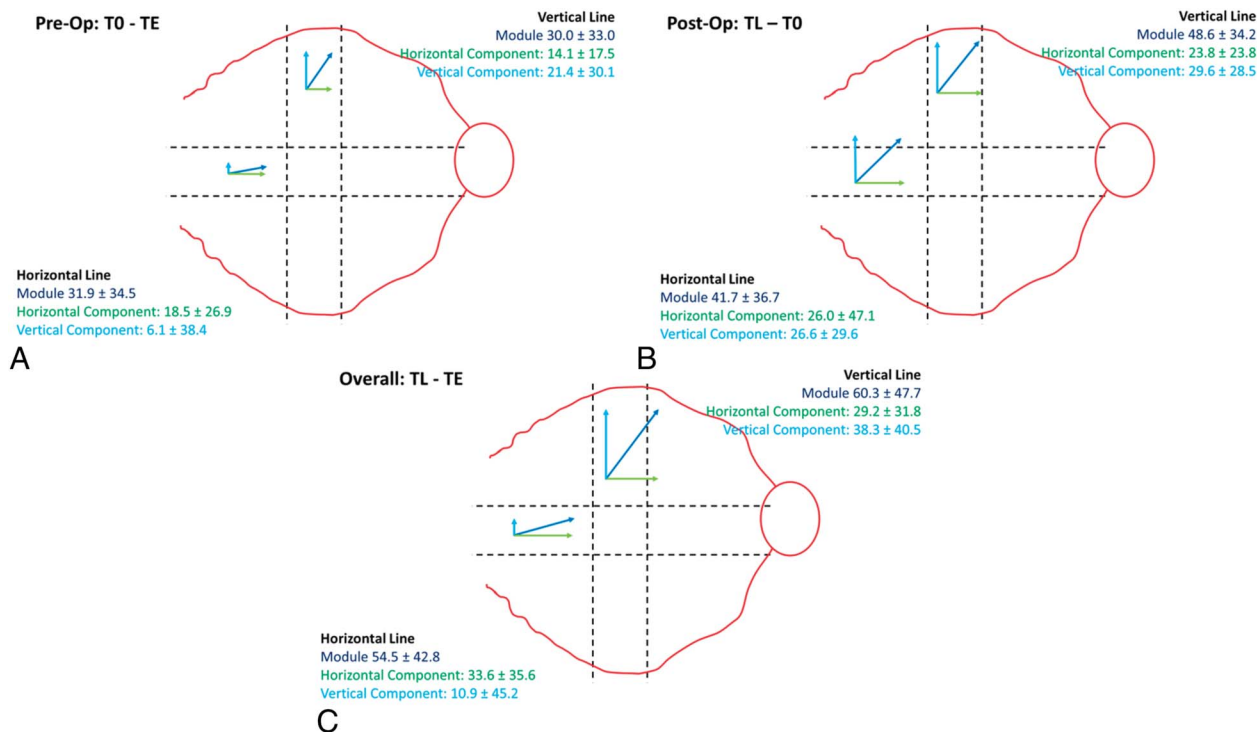


Fig. 5. Schematic drawing of the average macular dislocation vector decomposition across the orthogonal components in the (A) preoperative, (B) postoperative, and (C) overall follow-up period. Note how despite a similar average vector modulus, the horizontal and vertical components in the (A) $T_E - T_0$ and (B) $T_0 - T_L$ periods are differently represented, evidence of a significant increase in vertical displacement of the horizontal strip postsurgery.

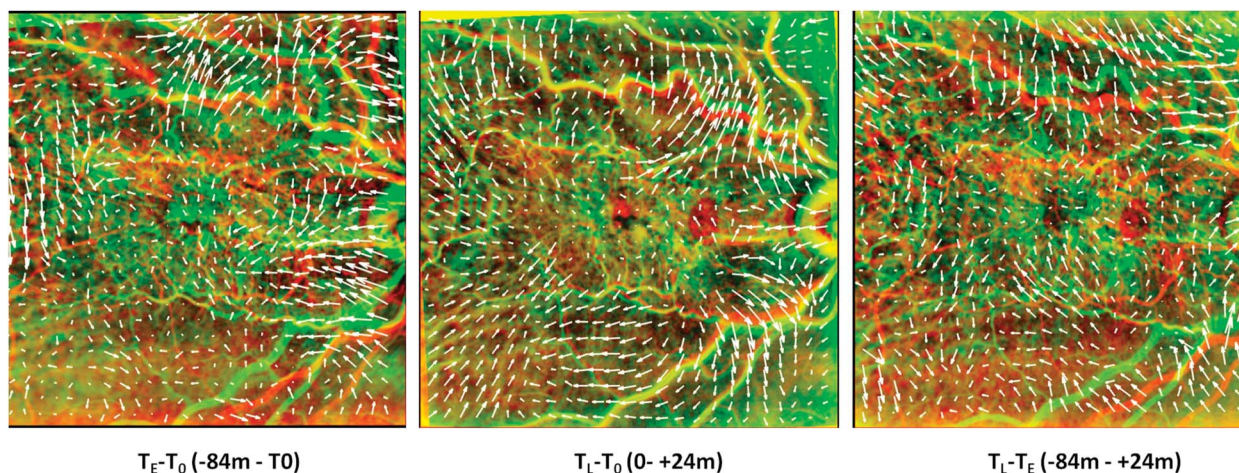


Fig. 6. Patient 31 displacement vectors. $T_0 - T_E$ (A) refers to the dislocation occurred between the earliest visit 84 months before surgical indication and immediately before surgery (T_0); note the erratic changes throughout the macula. $T_0 - T_L$ (B) shows the postoperative dislocation vectors between T_0 and 24 months after surgery; note how those vectors do not simply represent the opposite of the deformation occurred before surgery (A). $T_E - T_L$ (C) summarizes the entire preoperative and postoperative follow-up, spanning 9 years (108 months). The dislocation vectors show clearly how different retinal topography at the end of follow-up is, compared with T_E .

prone to deformation in the preoperative time ($T_E - T_0$; Table 4).

It is conceivable that the formation of ERMs^{20,21} may randomly contract the retinal surface and inner layers⁷ along any given axis, whereas the symmetric anatomy of the vascular arcades around the horizontal line transecting the fovea opposes to vertical distortion. Müller cells with their trans-retinal extension and specifically the stiff ILM²² would equally oppose to any applied force, regardless of orientation. This is consistent with our and Tung et al²³ observations, showing a prevalent foveal horizontal displacement vector between $T_E - T_0$ (i.e., before surgery, Figure 5). Indeed, this very resistance to tangential deformation, imposed by retinal stiffness, may be at least in part responsible for the functional decrease and explain the improvement after surgery, despite further tangential displacement and maybe thanks to it.

After surgery, in fact, ERM and ILM peeling releases internal retinal tension, and the structures are free to move in all directions, thus explaining the much greater representation of the tangential vertical component of dislocation vectors (Table 4, Figure 5). It should be noted that the ILM is almost invariably violated during ERM peeling, and large fragments of the Müller cells²⁴ peeled off even when the ILM is not deliberately removed, as is the case in this surgical series. Furthermore, most vital dyes themselves significantly alter the mechanical properties of the ILM.²⁵

In summary, we applied an already tested objective measure of retinal tangential displacement to ERM patients with a lengthy preoperative and postoperative follow-up, showing there is more dislocation after surgery than before and that functional improvement

does not necessarily correspond to anatomical or at least topographical restoration. We also were able to show the differential displacement of the foveolar and crosshair regions possibly related to a peculiar anatomy and maybe selected across the evolution of the visual system to preserve the foveal function from the consequences of inflammatory retinal wrinkling.

We accept that there are limitations to our study, including the use of infrared pictures that “flatten” all retinal details, thus losing the ability to consider the possible sliding of different retinal planes, and the fact itself that most “visible” details picked up by the image analysis algorithm are vessels, while other structures’ motion may be underrepresented or neglected. These areas are already the subject of ongoing research.

Key words: metamorphopsia, epiretinal membrane, macular pucker, retinal layer, retinal displacement.

Acknowledgments

The authors would like to thank the “Fondazione Roma” and the Italian Ministry of Health for financial support. The authors would also like to thank Giuliana Facciolo and Francesca Petruzzella for patient study and data gathering.

References

1. Simunovic MP. Metamorphopsia and its quantification. *Retina* 2015;35:1285–1291.
2. Romano MR, Cennamo G, Amoroso F, et al. Intraretinal changes in the presence of epiretinal traction. *Graefes Arch Clin Exp Ophthalmol* 2017;255:31–38.

3. Chang S, Gregory-Roberts EM, Park S, et al. Double peeling during vitrectomy for macular pucker: the Charles L. Schepens Lecture. *JAMA Ophthalmol* 2013;131:525–530.
4. Ichikawa Y, Imamura Y, Ishida M. Inner nuclear layer thickness, a biomarker of metamorphopsia in epiretinal membrane, correlates with tangential retinal displacement. *Am J Ophthalmol* 2018;193:20–27.
5. Sakai D, Takagi S, Hiram Y, et al. Correlation between tangential distortion of the outer retinal layer and metamorphopsia in patients with epiretinal membrane. *Graefes Arch Clin Exp Ophthalmol* 2021;259:1751–1758.
6. Scarinci F, Querzoli G, Cosimi P, et al. Retinal tectonics after macular pucker surgery: thickness changes and en-face displacement recovery. *Retina* 2023. Epub ahead of print.
7. Govetto A, Lalane RA 3rd, Sarraf D, et al. Insights into epiretinal membranes: presence of ectopic inner foveal layers and a new optical coherence tomography staging scheme. *Am J Ophthalmol* 2017;175:99–113.
8. Arimura E, Matsumoto C, Nomoto H, et al. Correlations between M-CHARTS and PHP findings and subjective perception of metamorphopsia in patients with macular diseases. *Invest Ophthalmol Vis Sci* 2011;52:128–135.
9. Parravano M, De Geronimo D, Scarinci F, et al. Progression of diabetic microaneurysms according to the internal reflectivity on structural optical coherence tomography and visibility on optical coherence tomography angiography. *Am J Ophthalmol* 2019;198:8–16.
10. Farnebäck G. Two-frame motion estimation based on polynomial expansion. In: Bigun J, Gustavsson T, eds. *Image Analysis. SCIA 2003. Lecture Notes in Computer Science*. Vol. 2749. Berlin, Heidelberg: Springer; 2003.
11. Arimura E, Matsumoto C, Okuyama S, et al. Retinal contraction and metamorphopsia scores in eyes with idiopathic epiretinal membrane. *Invest Ophthalmol Vis Sci* 2005;46:2961–2966.
12. Chua PY, Sandinha MT, Steel DH. Idiopathic epiretinal membrane: progression and timing of surgery. *Eye (Lond)* 2022;36:495–503.
13. Mieno H, Kojima K, Yoneda K, et al. Evaluation of pre- and post-surgery reading ability in patients with epiretinal membrane: a prospective observational study. *BMC Ophthalmol* 2020;20:95.
14. Amsler M. Earliest symptoms of diseases of the macula. *Br J Ophthalmol* 1953;37:521–537.
15. Ichikawa Y, Imamura Y, Ishida M. Metamorphopsia and tangential retinal displacement after epiretinal membrane surgery. *Retina* 2017;37:673–679.
16. Bringmann A, Unterlauff JD, Barth T, et al. Müller cells and astrocytes in tractional macular disorders. *Prog Retin Eye Res* 2022;86:100977.
17. Harada C, Mitamura Y, Harada T. The role of cytokines and trophic factors in epiretinal membranes: involvement of signal transduction in glial cells. *Prog Retin Eye Res* 2006;25:149–164.
18. Chen K, Weiland JD. Anisotropic and inhomogeneous mechanical characteristics of the retina. *J Biomech* 2010;43:1417–1421.
19. Govetto A, Hubschman JP, Sarraf D, et al. The role of Müller cells in tractional macular disorders: an optical coherence tomography study and physical model of mechanical force transmission. *Br J Ophthalmol* 2020;104:466–472.
20. Krishna Chandran AM, Coltrini D, Belleri M, et al. Vitreous from idiopathic epiretinal membrane patients induces glial-to-mesenchymal transition in Müller cells. *Biochim Biophys Acta Mol Basis Dis* 2021;1867:166181.
21. Kanda A, Noda K, Hirose I, Ishida S. TGF- β -SNAIL axis induces Müller glial-mesenchymal transition in the pathogenesis of idiopathic epiretinal membrane. *Sci Rep* 2019;9:673.
22. Henrich PB, Monnier CA, Loparic M, et al. Material properties of the internal limiting membrane and their significance in chromovitrectomy. *Ophthalmologica* 2013;230:11–20.
23. Tung HF, Chen YL, Tung HY, et al. Foveal displacement in eyes with epiretinal membrane after vitrectomy and membrane peeling. *Retina* 2021;41:2246–2252.
24. Díaz-Valverde A, Wu L. To peel or not to peel the internal limiting membrane in idiopathic epiretinal membranes. *Retina* 2018;38:S5–S11.
25. Haritoglou C, Mauell S, Benoit M, et al. Vital dyes increase the rigidity of the internal limiting membrane. *Eye (Lond)* 2013;27:1308–1315.